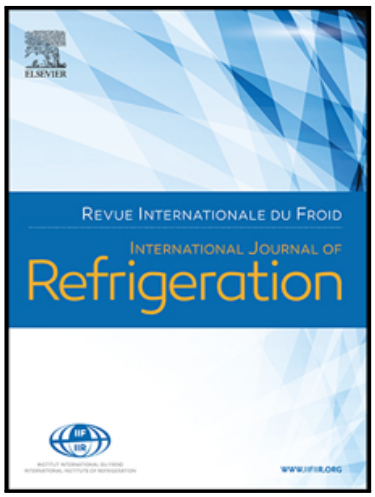

Energy evaluation of a Low Temperature commercial refrigeration plant working with the new low-GWP blend R468A as drop-in of R404A

Ramón Cabello , Daniel Sánchez , Rodrigo Llopis , Laura Nebot-Andrés , Daniel Calleja-Anta

PII: S0140-7007(21)00032-3
DOI: https://doi.org/10.1016/j.ijrefrig.2021.01.012
Reference: JIJR 5022

To appear in: *International Journal of Refrigeration*

Received date: 30 July 2020
Revised date: 15 January 2021
Accepted date: 16 January 2021

Please cite this article as: Ramón Cabello , Daniel Sánchez , Rodrigo Llopis , Laura Nebot-Andrés , Daniel Calleja-Anta , Energy evaluation of a Low Temperature commercial refrigeration plant working with the new low-GWP blend R468A as drop-in of R404A, *International Journal of Refrigeration* (2021), doi: https://doi.org/10.1016/j.ijrefrig.2021.01.012

Highlights

- First experimental work using R468A in a vapour compression cycle, mounting a low temperature freezing cabinet.
- Energy consumption is similar using R404A or R468A
- R468A is a proper energy alternative to R404A.
- No technical problems arise.
- IHX is useful to improve energy consumption when R468A is used as working fluid.

Energy evaluation of a Low Temperature commercial refrigeration plant working with the new low-GWP blend R468A as drop-in of R404A.

Ramón Cabello*, Daniel Sánchez, Rodrigo Llopis, Laura Nebot-Andrés, Daniel Calleja-Anta

Jaume I University, Dep. of Mechanical Engineering and Construction, Campus de Riu Sec s/n E-12071, Castellón, Spain

*Corresponding author: R. Cabello (cabello@uji.es), Phone: +34 964 72 8135; Fax: +34 964 728106.

ABSTRACT

This work analyses experimentally the energy behaviour of a centralized commercial refrigeration plant designed to be used with R404A (GWP_{100}=3,943) at low temperatures, when it is replaced with the new low-GWP refrigerant blend R468A (GPW_{100}=148). The tests have been done at a selected product temperature of -20ºC, Class III indoor conditions according to ISO 23953-2:2015 and 20, 30 and 40ºC of heat sink temperature. The product has been kept at the requested temperature in whichever conditions tested. Respect to R404A, running with R468A presents an increase in compressor discharge temperature, greater compression operation time, and a reduction in compressor electric comssumption that yields in a very similar total energy consumption of the refrigeration plant. So it has been proved that, from an operational point of view, R468A can be a R404A drop in replacement fluid. Also, it has been measured energy savings when an internal heat exchanger is placed.

KEYWORDS

R468A, R404A; IHX; drop-in; F-Gas, commercial refrigeration; energy analysis

NOMENCLATURE

COP	coefficient of performance
E	energy consumption, kW·h
GWP_{100}	Global warming potential, 100 years horizon
GWP_{20}	Global warming potential, 20 years horizon
h	specific enthalpy, $kJ \cdot kg^{-1}$
HR	relative humidity
IHX	Internal Heat Exchanger
$\dot{m}$	Mass Flow rate ($kg \cdot s^{-1}$)
NBP	Normal Boiling Point
ODP	Ozone Depleting Potential
p	pressure, (kPa)
P_C	power consumption, kW
$\dot{Q}_O$	cooling capacity, kW
q_o	Specific cooling capacity ($kJ \cdot kg^{-1}$)
SH	Superheating (ºC)
SC	Subcooling (ºC)
T	temperature, K/ºC
t	Time
v	Specific volume ($m^3 \cdot kg^{-1}$)
VCC	volumetric cooling capacity, $kJ \cdot m^{-3}$
x_v	vapour quality

GREEK SYMBOLS

λ	latent heat of phase-change, $kJ \cdot kg^{-1}$
Δ	Prefix, means preceding variable variation
η_v	Volumetric efficiency

SUBSCRIPTS

air	island return air to evaporator
c	Critical point
dis	Compressor discharge

suct	Compressor suction
in	Inlet
out	Outlet
sat,l	saturated liquid
o	evaporating level
k	condensing level
sat,v	saturated vapour

1. Introduction

Environmental rules are in progress all over the world. The refrigeration field is especially involved with those which affect fluorinated gases like EU517/2014 [1] in Europe, the Environmental Protection Agency's (EPA) Significant New Alternatives Policy (SNAP) in the US [2], the revised Recovery and Destruction of Fluorocarbons Act restrictions for Designated Products [3] in Japan or Kigali's Amendment on the Montreal Protocol [4] that is applied to the signatory countries. This concern is due to the fact that they affect the working fluids that the refrigeration facilities use. If we focus on commercial low-temperature applications, the fluids most commonly used until now are HFCs, specially R404A or R507A, with GWP_{100} values as high as 3,943 and 3,985, respectively.

The rules above mentioned stablishes restrictions in the quota of fluorinated gases production, given it in CO2 equivalent. So new alternative fluorinated gases with reduced GWP must be found, if it is intended to continue supplying the market with the necessary amount of this type of refrigerants. Apart from the natural refrigerants (organic and inorganic ones), the refrigerant manufacturers have made a big effort to produce new anthropogenic fluids that can be used as direct substitutes of HFC's. Thus, in the early 2000s, Dupont (currently Chemours) and Honeywell developed the R1234yf (2,3,3,3-Tetrafluoropropene), which was the first hydrofluoroolefin (HFO) marketed. This refrigerant was devised to replace the HFC134a in mobile air conditioning, to meet the European Directive 2006/40/EC.

HFOs constitute the new family of anthropogenic refrigerants. They are hydrofluorocarbons (HFCs) derived from propene with a short atmospheric lifetime, due to the instability conferred by unsaturated bounds. They are non-toxic, but the instability which generates very low GWP values (minor than 1 in general), on the contrary produces a light-middle flammability (2L classification according to ASHRAE Std34), so their use is limited in domestic and commercial applications.

Refrigerant manufacturers are developing many blends based on HFCs, HFOs and natural organic and inorganic fluids in order to meet the merits of the alternative fluids that will integrate the fourth generation of refrigerants: environmental acceptance (ODP=0, GWP as low as possible, preferable minor than 150), chemical stability in the refrigeration system, low toxicity and flammability, high efficiency and volumetric capacity.

In 2018 RTOC Assessment Report [5], published in 2019, stated that 35 new refrigerants, most of them blends, had been launched into the market since 2014. This proliferation of new refrigerants has been noticed in the latest editions of the reports made by refrigeration equipment manufacturers like Bitzer [6] or Danfoss [7], and in the most recent research articles (Domanski et al. [8], Belman et al. [9], Pave et al.l [10], Calleja-Anta et al. [11]). In Table 1 all the new alternative refrigerants found in literature with ASHRAE safety classification, and their main properties are gathered.

The rate at which these new refrigerants are appearing makes an experimental evaluation of many of them not available in the scientific literature. Accordingly, this work presents the experimental energy evaluation of one of the most recent marketed candidates to be a drop-in replacement option of R404A. This is the blend R468A, presented at the 25th ICR [2]. The analysis is done for a low-temperature application using a remote freezing island, and is divided into two main parts: first, a thermodynamic theoretical comparison about both refrigerants (Section 2) and, second, an energy comparison based on 24-hours tests carried out at different heat rejection levels (Section 4). The analysis has been restricted to energy parameters, so no environmental analysis has been performed.

Table 1 New refrigerants list

		MW (kg·kmol^{-1})	p_c (MPa)	T_c (K)	Safety Std34-2019	GWP_{20} /GWP_{100}	NBP vap.(K)	NBP Liq..(K)	VCC at NBP (kJ·m^{-3})
Non azeotropic mixtures									
R407G	R-32/125/134a (2.5/2.5/95.0)	100.0	4.146	372.6	A1	3,800 / 1,400	245.7	243.8	1,135
R407H	R-32/125/134a (32.5/15.0/52.5)	79.1	4.857	359.7	A1	3,800 / 1,500	235.3	228.3	1,138
R407I	R-32/125/134a (19.5/8.5/72.0)	86.9	4.614	365.3	A1	3,800 / 1,400	239.9	233.1	1,144
R436C	R-290/600a (95.0/5.0)	44.6	4.286	372.4	A3	1	233.2	231.4	1,018
R447B	R-32/125/1234ze(E) (68.0/8.0/24.0)	63.1	5.645	356.7	A2L	2,200 / 750	226.9	222.9	1,118
R449B	R-32/125/1234yf/134[a] (25.2/24.3/23.2/27.3)	86.4	4.531	355.3	A1	3,200 / 1,400	232.9	227.1	1,124
R449C	R-32/125/1234yf/134a (20.0/20.0/31.0/29.0)	90.3	4.398	357.4	A1	2,900 / 1,200	234.7	228.6	1,122
R452B	R-32/125/1234yf (67.0/7.0/26.0)	63.5	5.220	350.2	A2L	2,100 / 710	223.1	222.2	1,117
R452C	R-32/125/1234yf (12.5/61.0/26.5)	101.9	4.055	347.2	A1	4,100 / 2,200	228.8	225.4	1,110
R453A	R-32/125/134a/227ea/600/601a (20.0/20.0/53.8/5.0/0.6/0.6)	88.8	4.545	362.3	A1	4,100 / 1,700	237.9	230.2	1,139
R454A	R-32/1234yf (35.0/65.0)	80.5	4.627	354.9	A2L	890 / 250	230.7	225.0	1,102
R454B	R-32/1234yf (68.9/31.1)	62.6	5.267	351.3	A2L	1,700 / 490	223.4	222.4	1,115
R454C	R-32/1234yf (21.5/78.5)	90.8	4.319	358.8	A2L	540 / 150	235.1	227.3	1,104

R455A	R-744/32/1234yf (3.0/21.5/75.5)	87.5	4.654	358.8	A2L	540 / 150	233.7	220.8	1,124
R456A	R-32/134a/1234ze(E) (6.0/45.0/49.0)	101.4	4.175	375.8	A1	1,900 / 650	247.5	242.1	1,136
R457A	R-32/1234yf/152a (18.0/70.0/12.0)	87.6	4.308	363.2	A2L	520 / 150	237.3	230.3	1,105
R458A	R-32/125/134a/227ea/236fa (20.5/4.0/61.4/13.5/0.6)	89.9	4.527	365.2	A1	3,900 / 1,600	240.6	233.1	1,142
R459A	R-32/1234yf/1234ze(E) (68.0/26.0/6.0)	63.0	5.340	352.8	A2L	1,700 / 480	224.3	222.6	1,115
R459B	R-32/1234yf/1234ze(E) (21.0/69.0/10.0)	91.2	4.361	360.6	A2L	530 / 150	236.2	227.9	1,107
R460A	R-32/125/134a/1234ze(E) (12.0/52.0/14.0/22.0)	100.6	4.336	356.7	A1	4,100 / 2,100	236.2	228.2	1,131
R460B	R-32/125/134a/1234ze(E) (28.0/25.0/20.0/27.0)	84.8	4.890	361.2	A1	3,000 / 1,300	235.9	227.3	1,130
R460C	R-32/125/134a/1234ze(E) (2.5/2.5/ 46.0/49.0)	105.3	3.997	375.9	A1	2,000 / 730	248.4	245.0	1,128
R461A	R-125/143a/134a/227ea/600a (55.0/5.0/32.0/5.0/3.0)	109.6	3.793	353.4	A1	5,300 / 2,700	236.0	230.8	1,120
R462A	R-32/125/143a/134a/600 (9.0/42.0/2.0/44.0/3.0)	97.1	4.148	355.6	A2	4,700 / 2,200	236.0	229.5	1,130
R464A	R-32/125/1234ze(E)/227ea (27.0/ 27.0/40.0/6.0)	88.5	4.903	362.6	A1	2,700 / 1,300	237.4	226.6	1,126
R465A	R-32/290/1234yf (21.0/7.9/71.1)	82.9	4.336	354.9	A2	530 / 130	232.5	221.8	1,096
R466A	R-32/125/13I1 (49.0/11.5/39.5)	80.7	5.283	346.3	A1	1,891 / 696	219.1	218.9	1,108
R467A	R-32/125/134a/600a (22.0/5.0/72.4/0.6)	82.5	4.485	362.3	A2L	3,525 / 1,249	238.4	230.4	1,133
R468A	R-1132a/32/1234yf (3.5/21.5/75.0)	88.8	4.378	362.3	A2L	523 / 146	209.4	188.9	977
R469A	R744/R-32/R-125 (35.0/32.5/32.5)	59.1	6.598	330.2	A1	2,769 / 1,250	211.4	194.4	1,155
R470A	R744/32/125/134a/1234ze(E)/227 ea (10.0/17.0/19.0/7.0/44.0/3.0)	84.4	5.591	361.8	A1	1,992 / 909	237.3	210.2	1,188
Azeotropic mixtures									
R513B	R-1234yf/134a (58.5/41.5)	108.7	3.632	367.9	A1	1,600 / 560	243.3	243.2	1,092
R514A	R-1336mzz(Z)/1130(E) (74.7/25.3)	-	-	-	B1		-	-	-!
R515A	R-1234ze(E)/227ea	118.7	3.566	381.9	A1	630 /	254.1	254.1	1,104

	(88.0/12.0)					380			
R516A	R-1234yf/134a/152a (77.5/8.5/14.0)	102.6	3.615	369.8	A2L	400 / 140	243.5	243.4	1,078

2. Thermodynamic properties and theoretical performance

2.1 R404A vs R468A. Thermophysical properties comparison

The new refrigerant R468A is a non-azeotropic ternary blend of HFC32, HFO1234yf and HFO1132a, designed to replace R404A. The pure substances that conform the blend are all of the 4th generation of refrigerants, pointing to the novelty of the R468A. It was, indeed, included in ASHRAE Std 34 at the addenda y, dated on june 2019 [13].

It must be outlined that R468A is the first refrigerant that includes HFO-1132a as a component, also named 1.1-difluoroethylene or vinylidene fluoride. Up to now, HFO-1132a has been produced at large industrial scale as a starting monomer to make the fluoro-elastomer PVDF [12] [14]. Nowadays, because HFO-1132a is a compound which is formed during the production of HFO-1123 and HFO-1234yf as a byproduct [15], it has been identified as a refrigerant component. That is why HFC-1132a is one of the latest fluids added to ASHRAE std 34 [13] with A2 safety classification.

The main properties of this refrigerant compared to those of R404A are listed in Table 2.

Table 2 Refrigerants main properties

Refrigerant	**R404A**	**R468A**
Components[1]	HFC125 / HFC143a / HFC134a	HFC32 / HFO1234yf / HFO1132a
Composition (%weight) [1]	44 / 52 / 4	21.5 / 75 / 3.5
ODP[1]	0	0
GWP_{100} (AR5)[2]	3,943	146
GWP_{20} (AR5) [2]	6,582	545
Safety Class [1]	A1	A2L
Molecular Weight ($kg \cdot kmol^{-1}$)[1]	97.6	88.84
T_c (K / ºC) [1]	345.27 / 72.12	362.31 / 89.16
P_c (kPa / bar) [1]	3,750 / 37.50	4,378 / 43.78

ρ_c (kg·m^{-3})[1]	486.70	444.27
NBP $\left(\frac{K}{°C}\right)$ (liq. / vap.)	226.65 / 227.41 -46.50 / -45.74	210.02 / 236.82 -63.13 / -36.33
Glide$_o$ *[3]	0.657	24.5
Glide$_k$ **[3]	0.336	12.6
$v_{sat.v}$ (m^3·kg^{-1})*[3]	0.0932	0.1457
$v_{sat.l}$ (m^3·kg^{-1})*[3]	0.000780	0.000796
λ_o (kJ·kg^{-1})*[3]	190	246
λ_k (kJ·kg^{-1}) [3]**	120	171
VCC (kJ·m^{-3})* [3]	2,039	1,688

[1] ASHRAE Std 34 – 2019 ; [2] IPCC [16]; [3] Refprop v.10 [17]

*Calculated for a pressure corresponding to a temperature of 243K (-30°C) and x_v=0.5 (206 kPa in case R404A and 149 kPa in case R468A)

** Calculated for a pressure corresponding to a temperature of 313K (40°C) and x_v=0.5 (1.823 kPa in case R404A and 1.470 kPa in case R468A)

From the GWP values shown in Table 1 and Table 2, it can be concluded that R468A is included in the category of new alternative refrigerants to R404A complying with the environmental regulations, so it has been included into the low-GWP fluorinated refrigerants category [5]. R468A presents a global warming impact 12 times minor than R404A in a 20 years' time horizon, and 27 times minor in a 100 years time horizon. Moreover, because of its GWP_{100} value below 150, it is not penalized with the taxes that some countries have applied to greenhouse gases.

Otherwise, the environmental impact reduction is balanced with a light inflammability designed as A2L in ASHRAE std 34-2019. That characteristic is common in all other new low-GWP refrigerants (marked inTable 1 in red) and limits the refrigerant mass charged in the equipment. Safety regulations that affect to refrigeration equipment, like EN378. EN60335, ISO 5149 and IEC 60335, are revising its standards to increase the flammable refrigerant charge size limits and adapting them to the characteristics of this new sort of refrigerant. This will allow a higher charge, making possible A2L refrigerants to be used in a wide range of applications.

If we compare R468A molecular weight to that of R404A, the first is 9% "lighter", being it preferable to reduce the compressor energy losses across valves [18] and to get higher vaporization enthalpies. The critical temperature and pressure of R468A are greater than those of R404A. This fact implies that the

cycle will operate at lower reduced temperatures and pressures, generally resulting in higher efficiencies but lower volumetric capacity VCC and the requirement of a physically larger equipment [19].

The NBP of R468A value is low enough to assure the operation of the cycle over the atmospheric pressure, avoiding the possibility of air intake in the sealed circuit with the subsequent performance degradation of the heat exchangers, and generation of an explosion hazard in case of flammable refrigerants.

R468A presents a much greater glide in the whole saturation range, especially in the low-pressure region, around 20ºC, in front of the glide around 0.5ºC that presents R404A. If a proper glide matching is designed, the higher glide value could be an advantage to improve the heat transfer in the evaporator and condenser, resulting in a better cycle energy performance [20][21][22]. Conversely, it complicates the thermostatic control of the expansion valve, so makes it necessary to reprogram the electronic expansion valves with a fine new vapour saturation curve.

2.2 R404A vs R468A. Theoretical performance

To develop this section, a simple vapor compression cycle has been considered. The simulated cycle specifications represent the low temperature application conditions to which R468A and R404A are designed, and a wide range in heat sink temperatures. Those specifications are: evaporating temperature of -35ºC / 238K; condensing temperatures of 40ºC / 313K, 30ºC / 303K and 20ºC / 293K, no evaporator superheat nor condenser subcooling are set, pressure drop at refrigerant lines and heat exchangers have been disregarded as well as the heat losses/gains to/from the ambient, the compressor isentropic efficiency is assumed to be 100% and the internal heat exchanger efficiencies of 0% (no IHX) and 50%. To compare the mass flow rate driven by the compressor and its power consumption, a cooling capacity of 1000 W has been used as a reference.

For the parameters calculation, since R468A presents a large glide, the criteria recommended by ASERCOM [23] has been applied to calculate the phase change pressures from the given evaporation and condensing temperatures. This way, the condensing pressure has been evaluated for a vapour title of 50% and the given T_k as presented in Eq. (1), and the evaporating pressure using the average enthalpy value at the evaporator, Eq. (2). The variables about the specific cooling capacity, the refrigerant mass flow rate, the compressor work rate, the volumetric cooling capacity and the coefficient of performance are calculated using equations (3) to (7), respectively. All the thermodynamic properties were evaluated using Refprop v10.0 [17].

$$p_k = f(T_k, x_v = 0.5) \quad (1)$$

$$p_o = f\left(T_o, \frac{h_{o,in} + h_{sat.v}(p_o)}{2}\right) \quad (2)$$

$$q_o = h_{o,out} - h_{o,in} \quad (3)$$

$$\dot{m}_r = \frac{\dot{Q}_o}{q_o} \quad (4)$$

$$\dot{W}_C = \dot{m}_r \cdot (h_{dis} - h_{suct}) \quad (5)$$

$$VCC = \frac{q_o}{v_{suct}} \quad (6)$$

$$COP = \frac{q_o}{h_{dis} - h_{suct}} \quad (7)$$

In Figure 1, it is represented, in a pressure-enthalpy diagram, the simple vapour compression cycle. More data about the cycle energy performance at different heat sink temperatures and IHX efficiencies are shown in Table 3.

At a first glance, from Figure 1a and 1b, it can be observed that saturation pressures for R468A are lower than those for R404A at the same temperatures, especially at the evaporation region. Another observable issue is that the saturation dome is wider in case of R468A, mainly due to its greater vapour saturation enthalpies. When R468A is used , this characteristic, according to Table 3 data, generates, lower vapour quality at evaporator inlet (up to 15% less) and higher specific cooling capacities (higher than 60% without IHX, and higher than 70% with IHX, decreasing the increment in both cases as heat sink temperature goes down). Those properties, together with a good glide matching, aims to a better behaviour of R468A respect to R404A in the low-pressure region of the facility. The lower mass flow rate needed for the same cooling demand can cause the expansion valves to become larger, so a special account must be paid on that issue.

Figure 1a shows that the isentropic slope is lower in R468A and compression rates are higher which implies large specific compression work needed with respect to R404A. Counterbalancing these effects are the lower refrigerant mass flow rates can be found. The final result yields in a lower mechanical compressor power consumption using R468A for a given cooling demand and cycle conditions, as it is observed from data shown in Table 3 (the reduction ranges from 16.7% to 12.4% without IHX, and from 11.2% to 10.9% using 50% effectiveness IHX, being in both cases the reduction lower as the heat sink temperature decreases). The theoretical cycle thermal efficiency (COP) obtained for all the conditions shown in Table 3 is higher for R468A.

Regarding the compressor discharge temperature, it is slightly higher when the cycle is performed with R468A (up to 8K without IHX, and up to 5K with IHX).

It can be observed how R468A, compared with R404A and due to its higher critical point, accomplishes with the conclusions of the works published by McLinden and Domanski, as it works at lower pressure levels and presents higher energy efficiency but lower VCC [24], [25]. However, though working pressures are lower at the same phase change temperature/s for R468A than for R404A, the compression ratio is higher for R468A. The increment ranges without IHX from 17.9% to 11.7% and with IHX from 14.4 to 8.4%. Lower compression ratios correspond to lower heat sink temperatures. Lower VCC and higher compression ratio values indicate that the compressor may remain small in case of direct replacement of R404A with R468A. Special attention will be paid to that issue.

The effect of the IHX improves the energy performance in both refrigerants, but this improvement is more accentuated in R404A than in R468A, due to its higher subcooling degrees and lower impact of the superheating in the isentropic compression work.

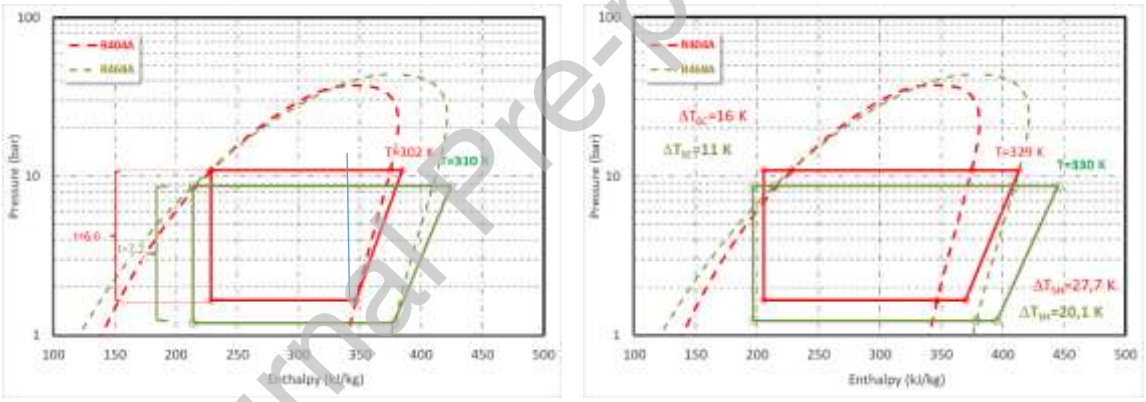

a) IHX efficiency 0% b) IHX efficiency 50%

Figure 1 R468A vs R404A. Theoretical vapour compression cycle comparison (T_k: 20ºC; T_o: -35ºC; isentropic efficiency: 1; null superheating and subcooling)

Table 3 Energy parameters obtained in theoretical vapour compression cycle (T_o: -35ºC; $\eta_{is.c}$: 1; ΔP: 0 kPa; SH: 0ºC; SC: 0ºC; $\dot{Q}_o = 1{,}000\ W$)

		IHX	P_o (kPa)	P_k (kPa)	$\dot{m}_r$ (g·s^{-1})	q_o (kJ·kg^{-1})	VCC (kJ·m^{-3})	$\dot{W}_C$ (W)	$x_{v,i}$ -	T_{dis} (K)	COP -
R468A	**T_k: 40ºC**	ε_{IHX}: 0%	114.9	1,478.6	7.7	130.0	697.9	464.8	0.403	332.6	2.15

		ε_{IHX}: 50%	118.6	1,478.6	6.3	157.7	754.1	439.9	0.288	364.5	2.27
	T_k: 30ºC	ε_{IHX}: 0%	117	1,142.6	6.8	147.4	804.9	363.5	0.330	321.2	2.75
		ε_{IHX}: 50%	120.8	1,142.6	5.9	169.9	847.8	351.7	0.239	347.2	2.84
	T_k: 20ºC	ε_{IHX}: 0%	119.8	867.4	6.1	164.3	917.5	281.1	0.261	309.7	3.56
		ε_{IHX}: 50%	123.6	867.4	5.5	181.6	950.8	275.4	0.194	329.7	3.63
R404A	**T_k: 40ºC**	ε_{IHX}: 0%	165.2	1,823.1	11.5	86.7	754.5	558.2	0.554	323.9	1.79
		ε_{IHX}: 50%	165.5	1,823.1	8.4	118.8	865.8	495.2	0.388	359.7	2.02
	T_k: 30ºC	ε_{IHX}: 0%	165.0	1,422.5	9.7	102.8	893.9	422.1	0.471	312.9	2.37
		ε_{IHX}: 50%	165.6	1,422.5	7.7	130.4	972.5	393.2	0.328	344.4	2.54
	T_k: 20ºC	ε_{IHX}: 0%	165.5	1,092.0	8.5	118.2	1,030.1	321.0	0.391	302.0	3.12
		ε_{IHX}: 50%	165.7	1,092.0	7.1	141.3	1,078.1	309.2	0.272	328.9	3.23

3. Experimental set-up description and test methodology.

3.1. Experimental set-up description

The experimental plant used for the evaluation of the refrigerant mixtures is schematized in Figure . The main components are: semi hermetic compressor (1), oil separator (2), brazed-plate condenser (3), liquid receiver (4), internal heat exchanger (IHX) (8), electronic expansion valve working as a thermostatic one (5), and finally, a finned-tube evaporator (6) installed inside a glass-door horizontal island for frozen food (7). Table 4 shows a detailed description of those components (dimensions, model, manufacturer…)

Table 4 Characteristics of the main components

Number	Component	Location	Main characteristics
1	Compressor	Machinery room	Semi hermetic compressor BITZER Model: 2HES-1Y-40S 6.5 $m^3 \cdot h^{-1}$ (1450 rpm) Lubricant oil: POE SL32
2	Oil separator	Machinery room	Hermetic oil separator ESK Model: OS-12 Volume: 2.3 dm^3
3	Condenser	Machinery room	Insulated brazed plate heat exchanger SWEP Model: B25-THX40 (40 plates) Heat transfer area: 2.39 m^2 Secondary fluid: water
4	Liquid receiver	Machinery room	Insulated liquid receiver TECNAC Volume: 5 dm^3
5	Expansion valve	Climatic chamber	Electronic expansion valve CAREL E2V11
6	Evaporator	Climatic chamber	Finned-tube heat exchanger from SEREVA. Tube of 3/8'' staggered array with fine spacing if 8 mm Heat transfer area (internal tube): 1.35 m^2
7	Freezing island	Climatic chamber	Horizontal island from FROST-TROL with glass doors. Dimensions: 1875 (L) x 1170 (H) x 1000 (W) mm Defrosting with electrical resistors: 2600 W
8	IHX	Climatic chamber	Inner tube heat exchanger PACKLESS Model: HXR-50 Heat transfer area (internal tube): 0.022 m^2
9	Product	Climatic chamber	M-test package (ISO-15502). Dimensions: 200 x 100 x 50 mm

Following the compressor manufacturer recommendation and due to operating conditions, additional cooling has been installed by means of a fan placed over the cylinder head. The energy consumption of this fan is the same in all tests and has been included in the energy analysis.

To control the external conditions, the freezing island is placed into a climatic chamber of 3 (L) x 3.5 (H) x 3 (W) m (31.5 m^3). This climatic chamber maintains Class III environmental conditions (25°C dry-bulb temperature; 60% RH) according to ISO 23953-2:2015.

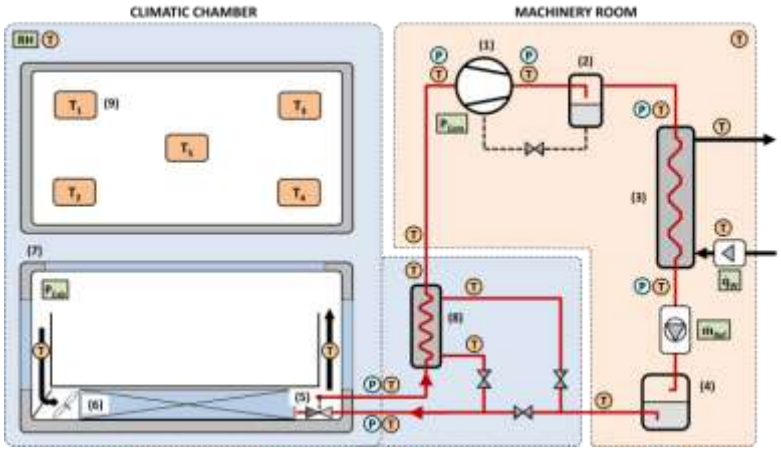

Figure 2 Schematic layout of the refrigeration system and measurement devices

To maintain the desired heat rejection conditions at the condenser, an external system is used as a heat sink. This external system controls the water inlet temperature and the volumetric flow rate by means of a refrigeration facility and electrical resistors. The power consumption of the pump that drives the water to the condenser has not been taken into account in the energy analysis.

3.2. Measurement system and uncertainties

The refrigerating facility schematized in Figure 2 is completely instrumented with different transducers as temperature and pressure probes, two flow meters, two watt-meters and one hygrometer. The aim of these transducers is to determine the thermodynamic states of the tested fluids and to calculate the heat transfer rate in the condenser or evaporator. Table 5 summarizes the calibration range and the accuracy of these measurement devices.

Table 5 Characteristics and accuracy of the measurement elements

Number	Variable	Type	Calibration range	Accuracy
21	Temperature	T-type thermocouple	-40 to 125 °C	± 0.5 °C
4	Pressure	Pressure gauge JOHNSON CONTROLS P499	0 to 30 bar	± 0.08 bar
3	Pressure	Pressure gauge JOHNSON CONTROLS P499	0 to 16 bar	± 0.04 bar
1	Mass flow rate	Coriolis flow meter YOKOGAWA ROTAMASS RCCT34	0 to 0.1 $kg \cdot s^{-1}$	± 0.1 % lecture
1	Volumetric flow rate	Magnetic flow meter YOKOGAWA RXF032G	0 to 2.5 $m^3 \cdot h^{-1}$	± 0.25 % lecture

1	Electric Power	Single phase digital Wattmeter SENECA Z203	0 to 3,000 W	± 0.5 % lecture
1	Electric Power	Three phases digital Wattmeter GOSSEN METRAWATT A210	0 to 2,500 W	± 0.5 % lecture
1	Dry-bulb temperature	Humidity and temperature transducer CAREL DPPC	-20 to 80 °C	± 0.5 °C
	Relative humidity		5 to 98 %	± 5 %

Data from sensors are acquired by two data acquisition systems CRio-9025 from National Instruments® with a time sampling of 5s. Thermophysical properties of the refrigerant and the secondary fluids are calculated with RefProp® v.10.0 and the software SecCool® v.1. The graphical interface to control the refrigeration facility has been developed with the software LabView®.

3.3. Test methodology

The evaporating process is controlled by an electronic expansion valve using an NTC sensor and a pressure gauge placed at the evaporator outlet. For an accurate superheating degree control of 15K, the valve driver has been upgraded with the vapor saturation curve of each tested refrigerant (R404A or R468A), using data from RefProp® v10.0.

The defrosting of the evaporator is made each 8 hours with electrical resistors (2,600 W). An NTC sensor placed over the finned surface measures the temperature to switching off the defrosting resistors when it reaches 5ºC.

The freezing island is placed at a climatic chamber where the inner conditions simulate the internal environment of the supermarket corresponding to Class III according to ISO 23953-2:2015. Internal environmental conditions are maintained constant for all the tests with standard deviations of ±0.2 K for temperature and 2.5 % for the relative humidity. This methodology guarantees that the same thermal loads are acting whichever the refrigerant used.

The freezing cabinet controller stops and closes the expansion valve when the air at the evaporator inlet reaches the selected value. This value (around -21ºC / -22ºC) is selected to keep the product at an average temperature of -20ºC. At the same time, the product average temperature is monitored using five thermocouples inserted in five packages distributed along and wide the freezing cabinet (see Figure 2)

The compressor has been running at a constant frequency of 1,500 rpm in all cycle conditions and tests. The governance strategy adopted to stop the compressor is an on/off regulation by means of a pressure switch installed at the compressor suction port. The pressure switch is adjusted to provide a low-cut temperature of -50°C (0.81 bar for R404A; 0.58 bar for R468A).

For each refrigerant, the plant has been charged with 4 kg and then, it is stabilized until the LT products reach the reference value (-20°C). At that moment the tests began. With the IHX disconnected, the tests length for each case has been of, at least, of 24 continuous hours including three defrosting periods. The tests with IHX have lasted for 16h of continuous running, including two defrosting periods.

As per the condenser, in order to take into account, the heat transfer process, the water inlet conditions are: temperature and mass flow rate are kept constant during the test for each outdoor conditions tested (20ºC, 30ºC and 40ºC)

Data of all the measurement devices were registered each 5 seconds (17,280 samples per sensor and test).

Table 6 and Table 7 summarize the averaged test conditions without IHX (24 hours) and with IHX (16 hours) at each condensing level. The standard deviation of each parameter is calculated and shown beside the corresponding mean value. It demonstrates the high stability of the measured parameters.

Two main conclusions arise from the data gathered at those tables. First, all test conditions are kept quite constant during their duration. Second, both refrigerants are capable of cooling and conserve the product at the desired frozen temperature.

Table 6 Test conditions summary without IHX (averaged during 24 hours)

Parameter	R404A			R468A		
Heat rejection temperature (°C)	20.2 ± 0.4	29.8 ± 0.6	39.9 ± 0.6	20.3 ± 0.3	30.0 ± 0.2	39.9 ± 0.2
Heat rejection flow rate ($m^3 \cdot h^{-1}$)	0.4 ± 0.003	0.4 ± 0.001	0.4 ± 0. 001	0.4 ± 0. 0030	0.4 ± 0. 0030	0.4 ± 0.001
Climatic chamber temperature (°C)	25.5 ± 0.2	25.5 ± 0.2	25.4 ± 0.2	25.4 ± 0.2	25.4 ± 0.2	25.4 ± 0.2
Climatic chamber relative humidity (%)	58.8 ± 2.1	59.0 ± 1.9	58.8 ± 2.1	58.6 ± 2.4	58.6 ± 2.5	58.5 ± 2.5
Average product temperature (°C)	-20.0 ± 0.4	-20.2 ± 0.5	-20.1 ± 0.5	-20.1 ± 0.7	-20.2 ± 0.5	-20.0 ± 0.6

Table 7 Test conditions summary with IHX (averaged during 16 hours)

Parameter	R404A			R468A		
Heat rejection temperature (°C)	20.1 ± 0.3	30.0 ± 0.7	39.8 ± 0.4	20.3 ± 0.3	30.2 ± 0.2	39.7 ± 0.2
Heat rejection flow rate ($m^3 \cdot h^{-1}$)	0.4 ± 0.001	0.4 ± 0.001	0.4 ± 0.001	0.4 ± 0.001	0.4 ± 0.001	0.4 ± 0.001
Climatic chamber temperature (°C)	25.5 ± 0.2	25.4 ± 0.2	25.6 ± 0.1	25.4 ± 0.2	25.6 ± 0.1	25.5 ± 0.2

Climatic chamber relative humidity (%)	58.6 ± 2.1	58.8 ± 1.7	59.1 ± 1.6	58.6 ± 2.6	59.1 ± 1.4	58.5 ± 2.5
Average product temperature (°C)	-20.2 ± 0.3	-20.1 ± 0.3	-19.9 ± 0.3	-20.0 ± 0.3	-20.0 ± 0.3	-20.2 ± 0.4

4. Energy consumption tests without IHX results.

In this section, the results obtained for the main energy parameters directly measured or calculated from data obtained in the tests made without IHX are analyzed and commented.

4.1. Cycle parameters

The values presented at this section have been averaged during the whole 24h test period only when the compressor is running.

The first cycle parameter commented is the compressor discharge temperature. The measured values are represented in Figure . From the graph, it is observed that R468A presents greater values in this parameter than R404A at the three heat sink temperatures assayed. The difference is below 10K in all cases. This difference agrees quite accurately with the theoretical values presented in Table 3.

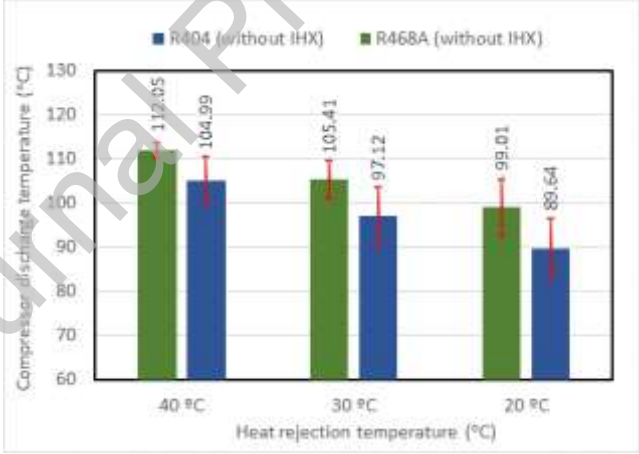

Figure 3 Compressor discharge temperature with standard deviation in measurements

As in the theoretical study, there is a great difference between the refrigerant mass flow rates, being R404A the fluid with higher values (7.5, 8.1 and 7.6 $g \cdot s^{-1}$) compared to those of R468A (5.2, 6.5 and 4.5 $g \cdot s^{-1}$). These mass flow rates correspond to 20ºC, 30ºC and 40ºC heat sink temperatures respectively.

Inlet pressures at the condenser and the evaporator are depicted in Figure 4 and Figure 5, respectively. According to the test methodology, each refrigerant presents quite constant average inlet evaporating pressures independently of the heat sink temperature, while inlet condenser pressures decreases with the

decrease of the heat sink temperature. Comparing pressures between refrigerants, there is no great difference at the condenser, although those of R468A are slightly greater than R404A ones. At the evaporator inlet, R404A presents higher pressure values than R468A.

At Figure 5, are also represented the average pressure losses at the evaporator. Comparing R404A pressure losses with R468A ones, the first ones are higher than the second ones, due to higher refrigerant mass flow rates associated with R404A. This fact makes that evaporator outlet pressures presents a minor difference between both refrigerants, in such way that the gap is reduced by half. So, inlet pressures and pressure losses at evaporator results in actual glide values around 9K for R468A and 5K for R404A. At condenser, pressure losses are negligible in both refrigerants.

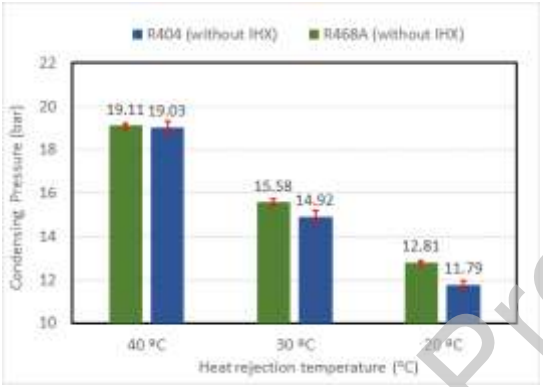

Figure 4 Inlet Condenser pressure with standard deviation in measurements

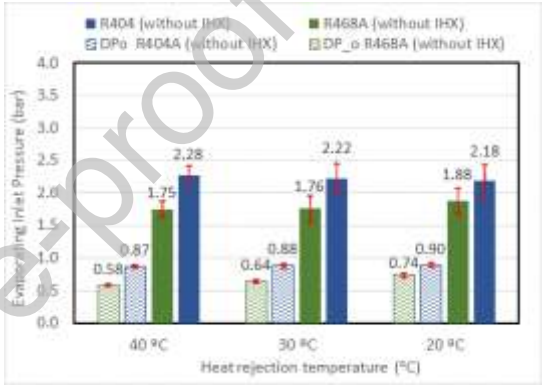

Figure 5 Evaporator inlet pressure with standard deviation in measurements

The lower pressure at evaporator result in higher compression ratios for R468A (13.7, 16.5 and 18.9) compared to R404A (11.4, 13.6 and 15.6) for the corresponding heat sink temperatures (20ºC, 30ºC and 40ºC).

In correspondence with the phase change pressures, the evaporating and condensing temperatures have been calculated according to ASERCOM recommendations [23]. In Figure are depicted those values. It can be observed that R468A condensing temperatures are seven degrees higher than R404A ones. However, the evaporating temperatures are two degrees higher for R468A than for R404A. This implies less irreversibility in the evaporation process for R468A. Two possible reasons may cause this effect. AT first, the pressure loss in the evaporator which contributes to the glide matching effect over the R468A. Secondly, the higher specific cooling capacity of R468A compared to R404A that enhances the evaporation process. This increment was ranged in Section 2 from 24 to 27%.

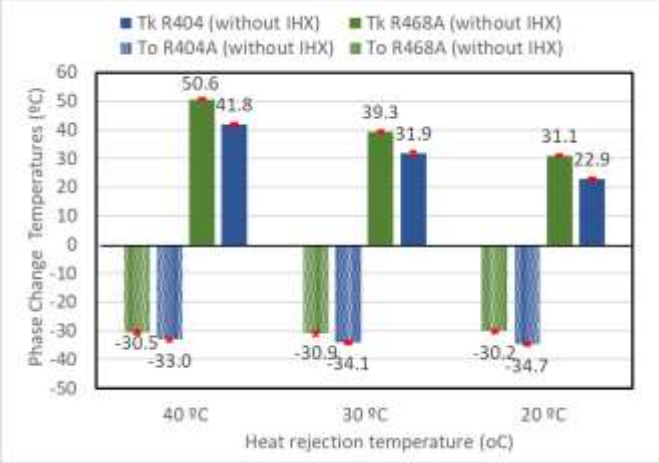

Figure 6 Phase change temperature (ºC)

The comparison between saturation temperatures and measured pressures at condenser and evaporator in both refrigerants, agrees with the results observed at the theoretical study Figures 1a and 3b.

The vapour quality at evaporator inlet is lower when using R468A than when using R404A (0.34, 0.39 and 0.43 in front of 0.37, 0.43 and 0.49 corresponding to heat sink temperatures 20ºC, 30ºC and 40ºC respectively). Moreover, R468A specific cooling capacities are significantly greater than those of R404A (an average ranging from 24% to 27%. This fact could justify a better evaporation process with R468A. This statement is corroborated by the fact that air is cooled with R468A from -20ºC to -28ºC, in average, compared to R404A, which cools air from -20ºC to -27ºC in average, despite working with lower evaporation temperatures.

4.2. Energy consumption parameters

This subsection begins with the analysis of the compressor and defrosting operating periods during the 24-hour test.

In Figure it is observed that compressor running time for both refrigerants is higher as heat sink temperature increases due to the increase in compressor ratio and the consequent results in the reduction of the volumetric efficiency.

R468A presents larger compressor running times with respect to R404A, from 3% at 20 heat sink temperature to 16% at 40ºC. This is mainly due to the higher specific volume of R468A and, therefore, its lower volumetric efficiency and volumetric cooling capacity compared to that of R404A.

In that sense we have estimated from measured values, that when the compressor works with R468A its volumetric efficiency ranges between 75% and 95% of that presented when it operates with R404A. The comparison has been calculated using Eq. 8.

$$\frac{\eta_{v\_R468A}}{\eta_{v\_R404A}} = \frac{\dot{m}_{ref} \cdot v_{suct.}|_{R468A}}{\dot{m}_{ref} \cdot v_{suct.}|_{R404A}} \quad (8)$$

The lower volumetric efficiency of R468A, not only lies on its higher specific volume, but also in its higher compression ratios stated in section 4.1.

The difference in compressor running time between both refrigerants makes greater as heat sink temperature increases. In fact, at 40ºC, the compressor working with R468A does not practically don't cycle during the test, but it should be remarked that the product remains at -20ºC. The reduction in volumetric cooling capacity was pointed at the theoretical analysis. However, in real conditions, it is evident that, despite this reduction and without increasing the compressor running frequency, the refrigeration plant working with R468A is able to keep the product at the target temperature.

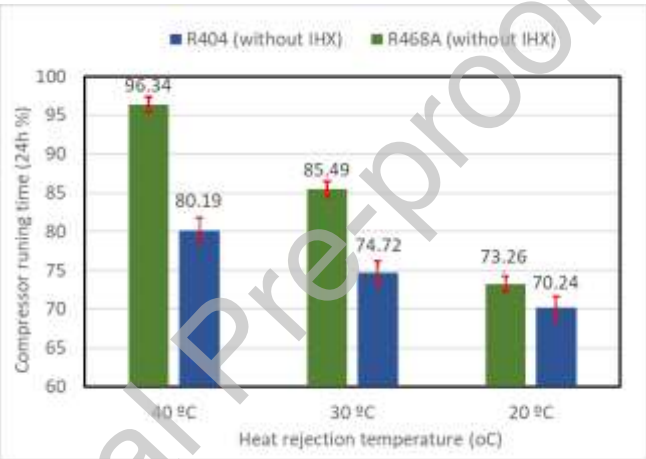

Figure 7 Compressor running time

Each 8 hours, a defrosting period starts and finishes when temperature at the evaporator surface reaches 5ºC. As Figure evidences, the refrigeration facility works with very similar defrosting times (between 10 and 12 min) regardless of the refrigerant used. This is reasonable due to the similar liquid densities (see Table 2), that generates similar inertias during the defrosting period.

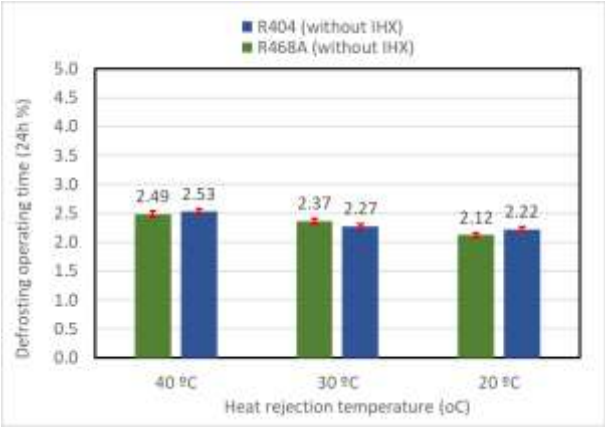

Figure 8 Defrosting operating time

While the compressor is running in each test, its average power consumption is depicted in Figure . The lower R468A mass flow rate allows the compressor to work with lower power consumption than when operating with R404A. This fact validates the result obtained with the theoretical study in section 2. The reduction ranges from 16% at 40ºC of heat sink temperature to 6% at 20ºC of heat sink temperature.

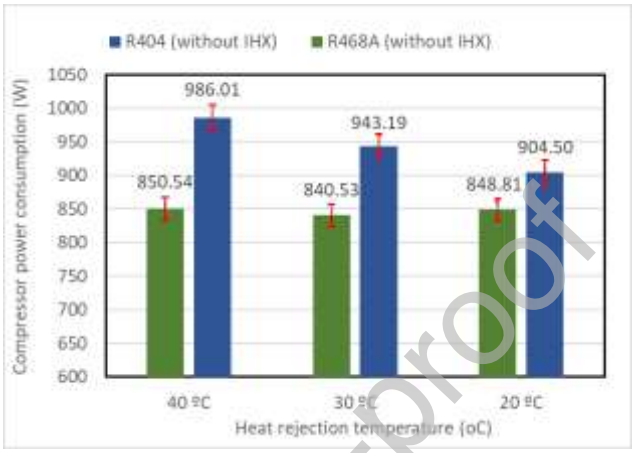

Figure 9 Average compressor power consumption

Finally, the total energy consumption of the facility during the 24-hour tests is shown in Figure 100. The energy consumption (kWh) of each element has been calculated from the power consumption measurements and operating time according to Eq. (9) using a trapezoid integration method. In Eq. (9), 'i' represents each energy consuming device (compressor, fan and freezing island), 'P_C' its corresponding power consumption and 'j' each sampled data. The difference between two samples is five seconds and the expression is evaluated during the 24-hour test.

$$E_i = \frac{1}{36 \cdot 10^5} \cdot \int_0^{24h} P_{C,i}(t) \cdot dt = \sum_{j=1}^{24h} \left[\frac{P_{C,i}(j) + P_{C,i}(j-1)}{2} \right] \cdot [t(j) - t(j-1)] \quad (9)$$

Taking into account that the compressor is the only component that presents different consumption values depending on the operating conditions and the refrigerant charged in the facility, the differences obtained at the total energy consumption are derived from the variation of the consumption in the compressor.

It can be stated from the data shown at Figure 100 that no significant differences are obtained from the energy consumption of the refrigeration plant when it charges R404A or R468A, showing very similar results.

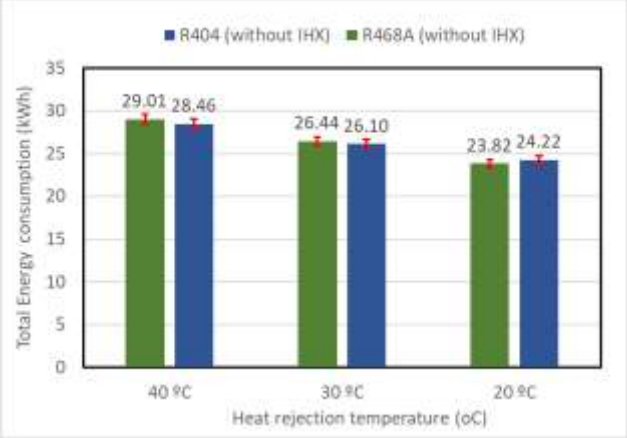

Figure 10 Refrigeration facility energy consumption during 24h tests

5. Energy consumption comparison when operating with and without IHX.

To conclude this work, the energy study of R468A in low temperature commercial refrigeration plants is completed with the analysis of the influence in the energy behaviour of an IHX placed at the evaporator outlet. The device installed is a concentric tube heat exchanger with counter current flow arrangement, placed beside the freezing island. Its aim is to put in thermal contact the expansion valve inlet and the evaporator outlet resulting in the cooling of the first and the heating of the second one.

This time, the tests have been carried out during a 16 hours period, in which two complete defrosting cycles have been done. Defrosting times are very similar than that obtained in 24h tests. Average test conditions, and corresponding standard deviations are collected in Table 7.

The internal heat transfer effectiveness ranges from 48% at 20ºC heat sink temperature test to 29% at 40ºC heat sink temperature.

In Figure 11, it can be observed that the compressor average discharge temperature suffers an increase of barely one Celsius degree. This is why, despite the 10K suction average temperature increase, the compressor working time is reduced enough to prevents its heating (see Figure 12) and the consequent increase in discharge temperature.

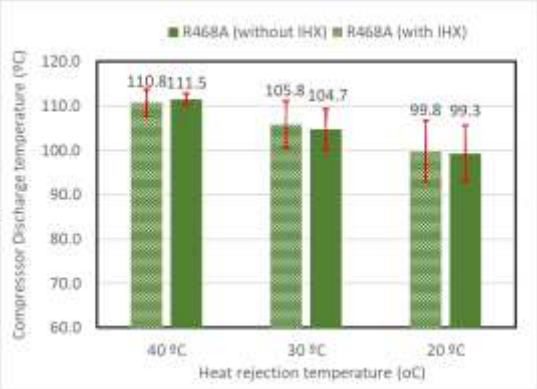

Figure 11 Compressor discharge temperature

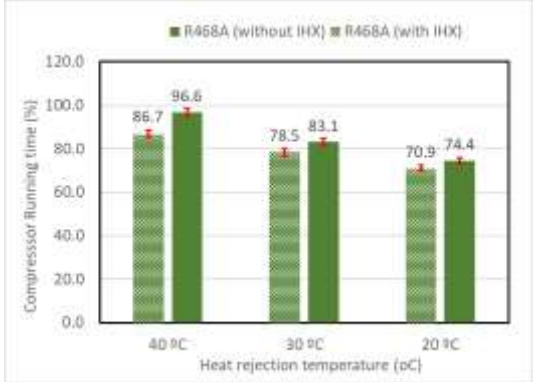

Figure 12 Compressor running time along 16h

Due to the additional subcooling provided at the IHX, the specific cooling capacity increases, which allows a significant reduction in the compressor working time. This is observed in Figure 12, where reductions are shown in a range of 3.5% to 10%. The reduction increases with the heat sink temperature, so it can be said that the IHX presents better results when higher is the ambient temperature.

The decrease in vapor quality at the evaporator inlet achieved when the internal heat exchanger is activated (increasing reductions from 5% to 9% as heat sink temperature increases), allows more energy absorption at the evaporator. Then, minor compressor running time (see Figure 13) is possible to eliminate the same cooling load at the freezing island. In consequence a reduction in the total energy absorbed by the refrigeration plant is obtained (Figure 14)

Once again, the best use of the IHX is revealed as the heat sink temperature increases, because in the face of the same increase in that temperature (from 20ºC to 40ºC), the increase in energy consumption is 2.2kWh when IHX is operating instead of 3.2kWh when it is off. That is, IHX dampens the effect of environmental temperature increase.

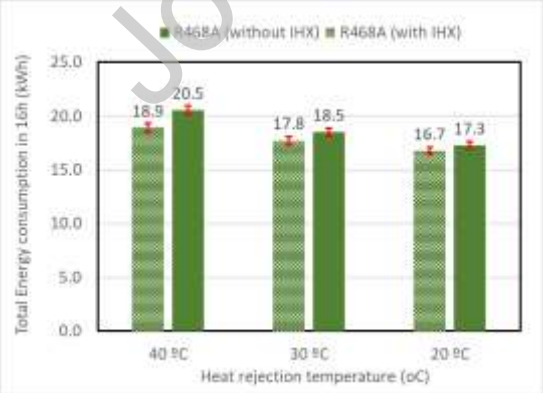

Figure 1 Average compressor electric power

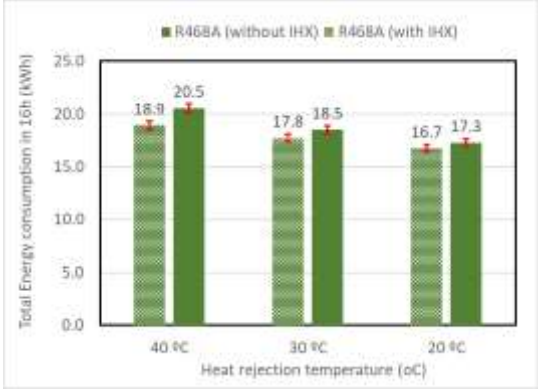

Figure 2 Total energy consumption in 16h test

6. Conclusions

This work has analyzed the actual energy behaviour of a low temperature commercial refrigeration plant working alternatively with R404A and R468A.

The refrigerant R404A replacement with R468A has been made without a need for changing any major system components, including lubricating oil, so R468A can be considered as a R404A drop in. For the proper thermostatic expansion valve operation, R468A vapor saturation curve has been provided to the regulator. A separate issue is the one related to the safety measures that could arise from the A2L safety classification of R468A, which are not treated in this work.

The discharge compressor temperature increases by 8 to 10K when the working fluid is R468A respect to R404A.

Evaporating conditions are favourable when the evaporator is fed with R468A respect to R404A. An increase in evaporating temperature, up to 2K, is achieved due to the minor vapour quality at the evaporator inlet and the glide matching that allows it to evaporate at a slightly higher temperature. Condensing temperatures are up to 7K higher when R468A is used.

Compared with R404A, compressor running time increases (up to 16%) when the plant is charged with R468A, but during this time its power consumption is lower (up to 14%). Those effects are counterbalanced in such a way that the energy consumed by the compressor and by the whole refrigeration plant are very similar to the range of conditions established in the tests.

Despite the reduction in volumetric efficiency, the commercial refrigeration plant operating with R468A is able to keep the product at the same low-temperature set with R404A, without the need to increase the compressor running frequency.

The introduction of an IHX placed at the freezing island allows the reduction of the total energy consumed in a quantity that ranges from 3% to 7%, without appreciable increase in the compressor discharge temperature.

7. Acknowledgements

The authors gratefully acknowledge the Ministerio de Ciencia y Tecnología – Spain (project RTI2018-093501-B-C21) and the Jaume I University (project UJI-B2019-56) for financing this research work.

Declaration of interests

The authors declare that they have no known competing financial interests or personal relationships that could have appeared to influence the work reported in this paper.

8. References

[1] M. Schulz and D. Kourkoulas, "Regulation (EU) No 517/2014 of the European Parliament and of the Council of 16 April 2014 on fluorinated greenhouse gases and repealing Regulation (EC) No 842/2006," *Off. J. Eur. Union*, 2014.

[2] C. Farquharson and G. McCarthy, "Protection of Stratospheric Ozone: New listings of substitutes; changes of listing status; and reinterpretation of unacceptability for closed cell foam products under the Significant New Alternatives Policy program; and revision of Clean Air Act Section 6," *Fed. Regist.*, 2016.

[3] G. of J. Ministry of the Environment, "Act on Rational Use and Proper Management of Fluorocarbons." 2016.

[4] UNEP, "The Kigali Amendment to the Montreal Protocol: HFC Phase-down," 2016.

[5] UNEP, "2018 Report of the Refrigeration, Air Conditioning and Heat Pumps Technical Options Committee." Ozone Secretariat, UNEP Nairobi, Kenya, p. 300, 2019.

[6] Bitzer, "Refrigerant Report 20," 2019.

[7] Danfoss, "Refrigerant options now and in the future," no. August, p. 24, 2018.

[8] P. A. Domanski, R. Brignoli, J. S. Brown, A. F. Kazakov, and M. O. McLinden, "Low-GWP refrigerants for medium and high-pressure applications," *Int. J. Refrig.*, 2017.

[9] J. J. García-pabón, "Overview of low GWP mixtures for the replacement of HFC refrigerants : R134a ," *Int. J. Refrig.*, vol. 111, pp. 113–123, 2019.

[10] P. MAKHNATCH, "New refrigerants for vapour compression refrigeration and heat pump systems," KTH Royal Institute of Technology, 2019.

[11] R. Calleja-Anta, D., Nebot-Andrés, L., Catalán-Gil, J., Sánchez, D., Cabello, R., & Llopis, "Thermodynamic screening of alternative refrigerants for R290 and R600a," *Results Eng.*, vol. 5, 2020.

[12] Y. K. Shun OHKUBO, Felix FLOHR, Kenji GOBOH, Tatsumi TSUCHIYA, Hitomi ARIMOTO, "The developing of lower GWP refrigerants," in *The 25th International Conference of Refrigeration*, 2019.

[13] ASHRAE, "Designation and Safety Classification of Refrigerants, Addendum y to ANSI/ASHRAE Standard 34-2019," *ANSI/ASHRAE Standard 34-2019*. ASHRAE, 2019.

[14] R. L. (Mexichem U. Ltd), "Evaluation of potential use of R1132A as a refrigerant blend component.," in *1st IIR International Conference on the Application of HFO Refrigerants*, 2018, p. 13.

[15] Y. TASAKA, Mai; FUKUSHIMA, Masato; KAWAGUCHI, Satoshi; TANIGUCHI, Tomoaki; TAKEUCHI, "WORKING MEDIUM FOR THERMAL CYCLE. EP 3 109 292 A1," EP 3 109 292 A1, 2015.

[16] M. G. . D. S. F. M. B. W. C. J. F. J. H. D. K. J.-F. L. D. L. B. M. T. N. A. R. G. S. T. T. and H. Zhang, *2013: The Physical Science Basis. Contribution of Working Group I to the Fifth Assessment Report of the Intergovernmental Panel on Climate Change*, 1st ed. London: Cambridge University Press, Cambridge, United Kingdom and New York, NY, USA., 2014.

[17] M. O. Lemmon, E.W., Bell, I.H., Huber, M.L., McLinden, "NIST Standard Reference Database 23: Reference Fluid Thermodynamic and Transport Properties-REFPROP, Version 10.0, National Institute of Standards and Technology, Standard Reference Data Program, Gaithersburg, 2018." 2018.

[18] W. D., "Factors affecting reciprocating compressor performance.," *Hydrocarb. Process.*, vol. 72, no. 6, 1993.

[19] J. S. McLinden, M.O., Domanski, P.A., Kazakov, A., Heo, J., Brown, "Possibilities, limits, and tradeoffs for refrigerants in the vapor compression cycle.," in *2012 ASHRAE/NIST Refrigerants Conference.*, 2012.

[20] E. Torrella, R. Cabello, D. Sánchez, J. A. Larumbe, and R. Llopis, "On-site study of HCFC-22 substitution for HFC non-azeotropic blends (R417A, R422D) on a water chiller of a centralized HVAC system," *Energy Build.*, vol. 42, no. 9, 2010.

[21] P. A. Marques, M.; Domanski, "Potential Coefficient of Performance Improvements Due to Glide Matching with R-407C.," in *International Refrigeration and Air Conditioning Conference*, 1998.

[22] M. P., M. B. A., and K. R., "The effect of temperature glide on the performance of refrigeration systems.," in *5th IIR Conference on Thermophysical Properties and Transfer Processes of Refrigerants.*, 2017, p. 8.

[23] ASERCOM, "Refrigerant Glide and Effect on Performances Declaration," no. September, pp. 1–11, 2015.

[24] I. H. Bell, P. A. Domanski, M. O. McLinden, and G. T. Linteris, "The hunt for nonflammable refrigerant blends to replace R-134a," *Int. J. Refrig.*, 2019.

[25] P. A. Domanski, R. Brignoli, J. S. Brown, A. F. Kazakov, and M. O. McLinden, "Frigorigènes à faible GWP pour les applications à moyenne et haute pression," *Int. J. Refrig.*, 2017.